John von Neumann Institute for Computing

The Pseudopotential Plane Wave Approach

Bernd Meyer

published in

Computational Nanoscience: Do It Yourself!,
J. Grotendorst, S. Blügel, D. Marx (Eds.),
John von Neumann Institute for Computing, Jülich,
NIC Series, Vol. **31**, ISBN 3-00-017350-1, pp. 71-83, 2006.

http://www.fz-juelich.de/nic-series/volume31

The Pseudopotential Plane Wave Approach

Bernd Meyer

Chair of Theoretical Chemistry
Ruhr-Universität Bochum
44780 Bochum, Germany
E-mail: bernd.meyer@theochem.rub.de

The pseudopotential plane wave approach has become one of the most widely used methods for calculating ground state properties of extended systems within the framework of density functional theory. The simplicity of plane waves leads to very efficient numerical schemes for solving the Kohn–Sham equations, and the employment of pseudopotentials guarantees that the wave functions can be expanded in a relatively small set of plane waves. In this article the basic expressions for plane–wave–based total energy calculations and a short overview of the different types of ab initio pseudopotentials will be given.

1 Introduction

In the previous chapters the complicated many–body problem of strongly interacting electrons and nuclei has been mapped within the framework of the Born–Oppenheimer approximation and density functional theory onto a problem of single–particles moving in an effective external potential for a set of fixed nuclei. Our aim now is to develop a practical numerical scheme to solve the resulting single–particle Kohn–Sham equations for extended systems like crystalline solids or liquids.

The most common approach to tackle this problem is to expand the single–particle eigenstates of the Kohn–Sham equations into a set of basis functions. The Schrödinger equation then transforms into an algebraic equation for the expansion coefficient which may be solved by various well–established numerical methods. In this chapter we will show that plane waves are a particular well suited set of basis functions for extended systems. Plane waves are the exact eigenfunctions of the homogeneous electron gas. Therefore, plane waves are the natural choice for a basis expansion of the electron wave functions for simple metals where the ionic cores can be viewed as rather small perturbations to the homogeneous electron gas ("nearly free electron" metals, see for example Ref. 1). Plane waves are orthonormal and energy–independent. Hence, upon a basis set expansion the Schrödinger equation transforms into a simple matrix eigenvalue problem for the expansion coefficients. A further advantage of plane waves is that they are not biased to any particular atom. Any region in space is treated on an equal footing so that calculations do not have to be corrected for a basis set superposition error. Since plane waves do not depend on the positions of the atoms, the Hellmann–Feynman theorem can be applied directly to calculate atomic forces. Even for a non-complete basis set the Pulay terms

are identical zero.

In practical calculations only plane waves up to a certain cutoff wave vector are included in the basis set. The convergence of the calculations with respect to the basis set size is therefore controlled by a single parameter and can be checked simply by increasing the length of the cutoff wave vector. However, due to the nodal structure of the valence wave

functions in the core region of the atoms a prohibitively large number of plane waves would be needed for a good representation of these fast oscillations. For plane wave approaches to be of practical use we have to replace the Coulomb potential of the electron–nucleus interaction by pseudopotentials. By introducing pseudopotentials we are able to achieve two goals: First, we can remove the core electrons from our calculations. The contribution of the core electrons to the chemical bonding is negligible but they contribute most to the total energy of the system (typically a thousand times more than the valence electrons). Hence, the removal of the core electrons from the calculation means that total energy differences between ionic configurations can be taken between much smaller numbers so that the required accuracy for the total energy calculations will be much less demanding than in an all–electron calculation. Second, by introducing pseudopotentials we replace the true valence wave functions by so-called pseudo wave functions which match exactly the true valence wave functions outside the ionic core region but are nodeless inside. These pseudo wave functions can be expanded using a much smaller number of plane wave basis states. A further advantage of pseudopotentials is that relativistic effects can be incorporated easily into the potential while further treating the valence electrons non–relativistically.

In spite of introducing pseudopotentials, the number of basis functions N_{pw} needed for an accurate calculation is still an order of magnitude larger than for approaches using localized orbitals. This disadvantage, however, is more than compensated by the possibility to evaluate many expressions with the help of the Fast Fourier Transform (FFT) algorithm. The most time consuming step in solving the single–particle Schrödinger equations is to apply the Hamilton operator to the valence wave functions. In a traditional matrix representation of the Hamilton operator this step scales quadratically with the number of basis functions. With plane waves and the FFT algorithm this operation reduces to a $N_{\mathrm{pw}} \ln(N_{\mathrm{pw}})$ scaling. Hence, for large systems the use of plane wave basis functions will become much more efficient than localized basis sets. Furthermore, the total charge density and the Hartree potential are easily calculated in a plane wave representation.

In Section 2 we will introduce the basic notation for describing infinitely extended periodic systems. This can only be a very brief summary. More details can be found in any textbook on solid state physics, for example in the books of Ashcroft and Mermin[1] or Kittel[2]. We will then show why it is useful to expand the valence wave functions using a basis set of plane waves. In Section 3 the basic ideas underlying present ab initio pseudopotentials will be given. More details on the plane wave pseudopotential method can be found in the extremely useful review articles of Denteneer and van Haeringen[3], Pickett[4], Payne et al.[5] and Marx and Hutter[6].

2 Why Using Plane Waves?

2.1 Supercells

Although we have simplified the complicated many–body problem of interacting electrons in the Coulomb potentials of fixed nuclei to a set of single–particle equations, the calculation of the one–electron wave functions for an extended (or even infinite) system is still a formidable task. To make the problem tractable we assume that our system of interest can be represented by a box of atoms which is repeated periodically in all three spacial directions. The box shall be described by three vectors $\mathbf{a}_1$, $\mathbf{a}_2$, and $\mathbf{a}_3$. The volume of the

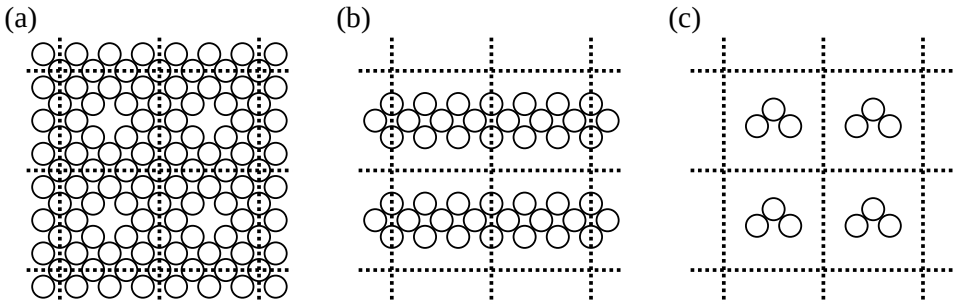

Figure 1. Schematic illustration of a supercell geometry (a) for a vacancy in a bulk crystalline solid, (b) for a surface, and (c) for a isolated molecule. The boundaries of the supercells are shown by dashed lines.

box is given by

$$\Omega_c = \mathbf{a}_1 \cdot (\mathbf{a}_2 \times \mathbf{a}_3) \quad . \tag{1}$$

The three vectors define a lattice in real space. General lattice vectors $\mathbf{T}$ are multiples of the primitive lattice vectors:

$$\mathbf{T} = N_1\mathbf{a}_1 + N_2\mathbf{a}_2 + N_3\mathbf{a}_3 \quad , \tag{2}$$

where N_1, N_2, N_3 can be any integer number. The box can be, for example, either the primitive unit cell of a crystal or a large supercell containing a sufficient number of independent atoms to mimic locally an amorphous solid or a liquid phase. By using supercells also atomic point defects, surfaces or isolated molecules can be modeled as illustrated schematically in Figure 1. It is essential to make the supercells large enough to prevent the defects, surfaces or molecules in neighboring cells from interacting appreciably with each other. The independence of the configurations can be checked systematically by increasing the volume of the supercell until the computed quantity of interest has converged.

2.2 Fourier Representations

The translational symmetry of the atomic arrangements can now be exploited to reduce the computational cost for solving the Kohn–Sham equations. The effective potential (as well as the electron density) is a periodic function with the periodicity of the lattice, i.e.

$$V_{\text{eff}}(\mathbf{r} + \mathbf{T}) = V_{\text{eff}}(\mathbf{r}) \tag{3}$$

for any lattice vector $\mathbf{T}$ of the form of Eq. (2). Therefore V_{eff} can be expanded into a Fourier series

$$V_{\text{eff}}(\mathbf{r}) = \sum_{\mathbf{G}} V_{\text{eff}}(\mathbf{G})\, \mathrm{e}^{i\mathbf{G}\mathbf{r}} \quad , \qquad V_{\text{eff}}(\mathbf{G}) = \frac{1}{\Omega_c} \int_{\Omega_c} V_{\text{eff}}(\mathbf{r})\, \mathrm{e}^{-i\mathbf{G}\mathbf{r}}\, \mathrm{d}^3\mathbf{r} \quad . \tag{4}$$

The sum runs over all vectors $\mathbf{G}$ which fulfill the condition $\mathbf{G} \cdot \mathbf{T} = 2\pi M$ for all lattice vectors $\mathbf{T}$ with M being an integer number. The vectors $\mathbf{G}$ form a lattice, the so-called reciprocal lattice, which is generated by the three primitive vectors $\mathbf{b}_1$, $\mathbf{b}_2$, $\mathbf{b}_3$ defined by[1]

$$\mathbf{a}_i \cdot \mathbf{b}_j = 2\pi\, \delta_{ij} \quad , \qquad i, j = 1, 2, 3 \quad . \tag{5}$$

The volume of the unit cell of the reciprocal lattice is given by

$$\mathbf{b}_1 \cdot (\mathbf{b}_2 \times \mathbf{b}_3) = \frac{(2\pi)^3}{\Omega_c} \quad . \tag{6}$$

2.3 Bloch's Theorem

The solutions of a single–particle Schrödinger equation with a periodic potential are by no means themselves necessarily periodic. However, the eigenstates can be chosen in such a way that associated with each wave function ψ is a wave vector $\mathbf{k}$ to hold

$$\psi(\mathbf{r} + \mathbf{T}) = \mathrm{e}^{i\mathbf{k}\mathbf{T}}\, \psi(\mathbf{r}) \tag{7}$$

for every lattice vectors $\mathbf{T}$ (Bloch's theorem[1]). From now on all eigenstates of the single–particle Schrödinger equation will be labeled with its corresponding vector $\mathbf{k}$. From the form of the exponential factor in Eq. (7) it is obvious that the values of $\mathbf{k}$ can be restricted to within one unit cell of the reciprocal lattice. By convention this unit cell is usually taken to be the first Brillouin zone (BZ)[1]. Different solutions to the same vector $\mathbf{k}$ will be labeled with the band index j.

Bloch's theorem is often stated in an alternative form. The property in Eq. (7) is equivalent to the statement that all eigenfunctions $\psi_{\mathbf{k}j}$ of a single–particle Schrödinger equation with a periodic potential can be written as a periodic function $u_{\mathbf{k}j}$ modulated by a plane wave with wave vector $\mathbf{k}$[1]:

$$\psi_{\mathbf{k}j}(\mathbf{r}) = \mathrm{e}^{i\mathbf{k}\mathbf{r}}\, u_{\mathbf{k}j}(\mathbf{r}) \quad . \tag{8}$$

This allows us to restrict the calculation of the eigenfunctions to within one unit cell. The form of the eigenfunctions in all other unit cells is determined by applying Eq. (7). From now on we will assume that the eigenfunctions are normalized with respect to a single unit cell:

$$\int_{\Omega_c} |\psi_{\mathbf{k}j}(\mathbf{r})|^2 \, \mathrm{d}^3\mathbf{r} = 1 \quad . \tag{9}$$

Since the functions $u_{\mathbf{k}j}$ are periodic they can be expanded in a set of plane waves. Together with the exponential prefactor we get:

$$\psi_{\mathbf{k}j}(\mathbf{r}) = \sum_{\mathbf{G}} c_{\mathbf{G}}^{\mathbf{k}j}\, \mathrm{e}^{i(\mathbf{k}+\mathbf{G})\mathbf{r}} \quad . \tag{10}$$

Before we make use of the plane wave expansion of the wave functions we write the Kohn–Sham equations of density functional theory in the notation of Bloch–states:

$$\left(-\frac{\hbar^2}{2m}\Delta + V_{\mathrm{eff}}(\mathbf{r})\right) \psi_{\mathbf{k}j}(\mathbf{r}) = \varepsilon_{\mathbf{k}j}\, \psi_{\mathbf{k}j}(\mathbf{r}) \tag{11}$$

with

$$V_{\mathrm{eff}}(\mathbf{r}) = V_{\mathrm{ext}}(\mathbf{r}) + V_{\mathrm{H}}[n(\mathbf{r})] + V_{\mathrm{xc}}[n(\mathbf{r})] \tag{12}$$

and

$$n(\mathbf{r}) = 2\,\frac{\Omega_c}{(2\pi)^3} \sum_j \int_{\mathrm{BZ}} |\psi_{\mathbf{k}j}(\mathbf{r})|^2 \; \Theta(E_{\mathrm{F}} - \varepsilon_{\mathbf{k}j})\, \mathrm{d}^3\mathbf{k} \quad . \tag{13}$$

$V_{\rm ext}$, $V_{\rm H}$ and $V_{\rm xc}$ are the external potential of the nuclei, the Hartree and the exchange–correlation potential, respectively. By the factor of 2 in Eq. (13) we take the electron spin into account. Θ is a step function which is one for positive and zero for negative arguments. $E_{\rm F}$ is the Fermi energy up to which single–particle states have to be occupied. The Fermi energy is defined by the number of electrons N_e in the unit cell:

$$\int_{\Omega_c} n(\mathbf{r})\,\mathrm{d}^3\mathbf{r} = N_e \quad . \tag{14}$$

For an insulator the Fermi energy lies in a band gap. Hence, at each k–point exactly $N_e/2$ bands will be occupied. For metals one or more bands cross the Fermi energy so that the number of occupied states will change between k–points.

2.4 k–Point Sampling

By making use of Bloch's theorem we have transformed the problem of calculating an infinite number of electronic states extended infinitely in space to one of calculating a finite number of eigenstates at an infinite number of k–points which are extended over a single unit cell. At first glance this seems to be only a minor improvement since still an infinite number of calculations are needed for the different k–points. However, the electronic wave functions at k–points which are close together will be very similar. Hence it is possible to represent the wave functions of a region of k–space by the wave function at a single k–point. We thus define a regular mesh of $N_{\rm kpt}$ k–points and replace the integral over the Brillouin zone by a discrete sum over the chosen k–point mesh:

$$\frac{\Omega_c}{(2\pi)^3}\int_{\rm BZ} \ldots\ \Theta(E_{\rm F}-\varepsilon_{\mathbf{k}j})\,\mathrm{d}^3\mathbf{k} \qquad \longrightarrow \qquad \frac{1}{N_{\rm kpt}}\sum_{\mathbf{k}} f_{\mathbf{k}j}\ \ldots \tag{15}$$

The $f_{\mathbf{k}j}$ are occupation numbers which are either one or zero. Several schemes to construct such k–point meshes have been proposed in the literature[7–9]. Within this approximation the electronic states at only a finite number of k–points are needed to calculate the charge density and hence the total energy of the solid. The error induced by this approximation can be reduced systematically by increasing the density of the k–point mesh. For insulators it turns out that usually only a small number of k–points is required to get good converged results. For increasing size of the supercell the volume of the Brillouin zone becomes smaller and smaller (see Eq. (6)). Therefore, with increasing supercell size less and less k–points are needed. From a certain supercell size on it is often justified to use just a single k–point, which is usually taken to be $\mathbf{k}$=0 (Γ–point approximation). For metallic systems, on the other hand, much denser k–point meshes are required in order to get a precise sampling of the Fermi surface. In these cases the convergence with respect to the k–point density can often be accelerated by introducing fractional occupation numbers[10–13].

2.5 Jellium Model

Why is it reasonable to expand the electronic wave functions using a basis set of plane waves? Let us first consider the very simple example of the jellium model (also called the Sommerfeld theory of metals[1]). In this model only the valence electrons are considered and the charges of the remaining ionic cores are assumed to be spread out into a uniform

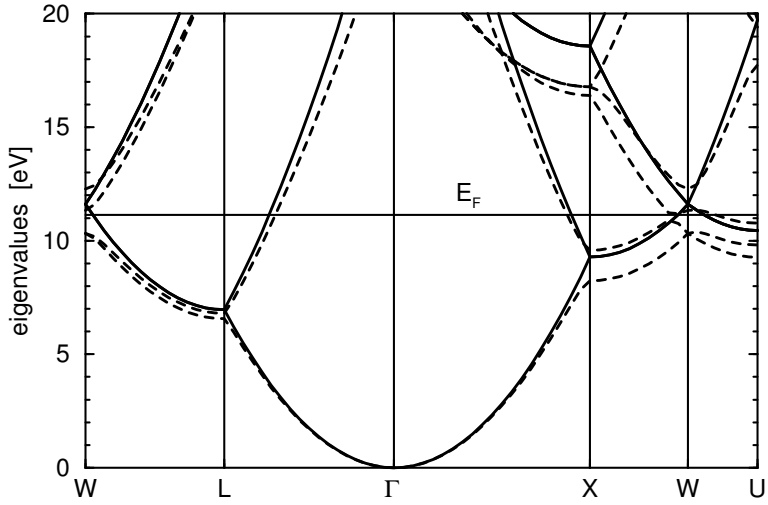

Figure 2. Band structure for a jellium model assuming the valence electron density and the cubic face–centered lattice of the "nearly–free electron" metal Al (solid line). The corresponding band structure of a full DFT calculation is shown by dashed lines. The energy levels are plotted along some high symmetry lines in the first Brillouin zone. The horizontal line indicates the Fermi energy.

positive background distribution. The external effective potential becomes constant and is set to zero. For the jellium model the Kohn–Sham equations can be solved easily. The eigenstates of the single–particle Schrödinger equation

$$-\frac{\hbar^2}{2m}\Delta\psi^{\rm jel}_{\mathbf{k}j}(\mathbf{r}) \;=\; \varepsilon^{\rm jel}_{\mathbf{k}j}\,\psi^{\rm jel}_{\mathbf{k}j}(\mathbf{r}) \tag{16}$$

are plane waves to a single reciprocal lattice vector $\mathbf{G}_j$ with the eigenvalues describing a simple quadratic dispersion relation:

$$\psi^{\rm jel}_{\mathbf{k}j}(\mathbf{r}) = \frac{1}{\sqrt{\Omega_c}}\,\mathrm{e}^{i(\mathbf{k}+\mathbf{G}_j)\mathbf{r}} \quad , \qquad \varepsilon^{\rm jel}_{\mathbf{k}j} = \frac{\hbar^2}{2m}||\mathbf{k}+\mathbf{G}_j||^2 \quad . \tag{17}$$

The labeling of the reciprocal lattice vectors $\mathbf{G}_j$ is done in such a way that the eigenvalues are in increasing order with increasing band index j. With these solutions the electron density becomes constant, and the Fermi energy is given by:

$$n(\mathbf{r}) = \frac{N_e}{\Omega_c} \quad , \qquad E_{\rm F} = \frac{\hbar^2}{2m}\left(3\pi^2\frac{N_e}{\Omega_c}\right)^{2/3} \quad . \tag{18}$$

In Figure 2 the band structure of the jellium model is shown for a cubic face–centered lattice (fcc) assuming the unit cell volume and the number of valence electrons of Al. The folding of the free–electron parabola into the Brillouin zone of the fcc lattice already creates a surprisingly complex band structure. Note that some of the energy bands are highly degenerate since sometimes several different reciprocal lattice vectors lead to the same eigenvalue.

2.6 Nearly Free Electrons

If we assume that the true external potential of the ionic cores of the atoms represents only a weak perturbation to the jellium model, then, taking the arguments from perturbation theory, it would be quite natural to describe the corresponding wave functions by a linear combination of a few plane waves, and the band structure should deviate not too much from the jellium result. Thinking of the Coulomb–nature of the ionic core potentials this seems to be not a very realistic assumption. However, comparing the true band structure of Al from a full DFT calculation with the free electron bands in Figure 2 reveals a surprising agreement. Some of the degeneracies of the free electron bands are lifted, but overall there is a rather close match between the two calculations.

How can this be understood? Though the eigenvalues are very similar, the corresponding eigenfunctions are quite different. In the jellium calculation they are nodeless single plane waves. In the full DFT calculation, on the other hand, the valence wave functions are composed of the $3s$ and $3p$ Al valence orbitals with nodes and fast oscillations in the ionic core region. These nodes and oscillations are due to the requirement that the valence wave functions are orthogonal to the core state. Effectively this leads to a repulsion of the $3s$ and $3p$ electrons from the core region (which can be viewed as a Pauli repulsion) so that overall the ionic core of the Al atom indeed behaves more like a weak perturbation for the valence electrons. However, the nodes and oscillations of the valence wave functions are restricted to the small ionic core region. Outside they match rather well the plane waves of the jellium calculation. Hence it should be possible to replace the ionic core potential by a much weaker potential that reproduces exactly the true wave functions outside the core region to the same eigenvalues, but with nodeless wave functions inside the ionic core. This is the original idea of introducing pseudopotentials. In the first applications pseudopotentials were constructed by explicitly projecting out the core electron contributions (so-called Phillips–Kleinman pseudopotentials[14]) or were purely empiric[15]. Today pseudopotentials are constructed from ab initio calculations for isolated atoms. We will come back to this point in the next section where we introduce pseudopotentials from a slightly different point of view. For the moment we will just assume that we can always introduce an appropriate pseudopotential so that the corresponding pseudo wave functions can be represented by a small set of plane waves.

2.7 Fourier Representation of the Kohn–Sham Equations

In a plane wave representation of the wave functions the Kohn–Sham equations assume a particular simple form. If we insert Eq. (10) into Eq. (11), multiply from left with $\exp(-i(\mathbf{k}+\mathbf{G}')\mathbf{r})$ and integrate over $\mathbf{r}$ we get the matrix eigenvalue equation

$$\sum_{\mathbf{G}} \left(\frac{\hbar^2}{2m} ||\mathbf{k}+\mathbf{G}||^2 \delta_{\mathbf{G}'\mathbf{G}} + V_{\text{eff}}(\mathbf{G}'-\mathbf{G}) \right) c_{\mathbf{G}}^{\mathbf{k}j} = \varepsilon_{\mathbf{k}j}\, c_{\mathbf{G}'}^{\mathbf{k}j} \quad . \tag{19}$$

In practical calculations the Fourier expansion (Eq. (10)) of the wave functions is truncated by keeping only those plane wave vectors $(\mathbf{k}+\mathbf{G})$ with a kinetic energy lower than a given cutoff value E_{pw}:

$$\frac{\hbar^2}{2m} ||\mathbf{k}+\mathbf{G}||^2 \leq E_{\text{pw}} \quad . \tag{20}$$

The convergence of all calculations with respect to the basis set size can be tested simply by increasing step by step the plane wave cutoff energy.

The electron density in Fourier representation is given by

$$n(\mathbf{G}) = \frac{2}{N_{\mathrm{kpt}}} \sum_{\mathbf{k}j} f_{\mathbf{k}j} \sum_{\mathbf{G}'} \left(c^{\mathbf{k}j}_{\mathbf{G}'-\mathbf{G}} \right)^* c^{\mathbf{k}j}_{\mathbf{G}'} \quad . \tag{21}$$

Since we have truncated the wave functions at a maximum wave vector it is obvious from Eq. (21) that the electron density has only non-vanishing Fourier components up to twice the length of this cutoff wave vector. In Fourier space the calculation of the Hartree potential is particularly simple. It is given by

$$V_{\mathrm{H}}(\mathbf{G}) = 4\pi e^2 \frac{n(\mathbf{G})}{||\mathbf{G}||^2} \quad . \tag{22}$$

As the electron density, the Hartree potential has a finite Fourier expansion. To calculate the exchange–correlation potential we have to Fourier transform the electron density to real–space, evaluate the given functional and Fourier transform back the result.

2.8 Fast Fourier Transformation (FFT)

The main advantage of working with plane waves is that the evaluation of various expressions can be speeded up significantly by using FFTs. In particular, since the wave functions and the electron density have a finite Fourier representation this can be done without any loss in accuracy, as long as we use in our real–space Fourier grid twice as many grid points in each spacial direction than the number of points in the Fourier space grid[16]. For example, the calculation of the electron density according to Eq. (21) scales quadratically with the number N_{pw} of plane waves. However, if we Fourier transform the wave functions to real–space (which scales with $N_{\mathrm{pw}} \ln(N_{\mathrm{pw}})$), calculate $|\psi_{\mathbf{k}j}(\mathbf{r})|^2$ on the real–space Fourier grid (N_{pw} scaling) and then Fourier transform back the result we significantly reduce the computational cost. Along the same arguments we can also reduce the number of calculations for the evaluation of the term $\sum_{\mathbf{G}} V_{\mathrm{eff}}(\mathbf{G}' - \mathbf{G}) c^{\mathbf{k}j}_{\mathbf{G}}$ in Eq. (19) from a N^2_{pw} to a $N_{\mathrm{pw}} \ln(N_{\mathrm{pw}})$ scaling.

3 Pseudopotentials

3.1 Frozen–Core Approximation

Most physical and chemical properties of crystals depend to a very good approximation only on the distribution of the valence electrons. The core electrons do not participate in the chemical bond. They are strongly localized around the nucleus, and their wave functions overlap only very little with the core electron wave functions from neighboring atoms. Therefore, the distribution of the core electrons basically does not change when the atoms are placed in a different chemical environment. It is thus justified to assume the core electrons to be “frozen” and to keep the core electron distribution of the isolated atom in the crystal environment.

The first advantage of the frozen–core approximation is that now less electrons have to be treated and less eigenstates of the Kohn–Sham equations have to be calculated. The second advantage is that the total energy scale is largely reduced when the core electrons are

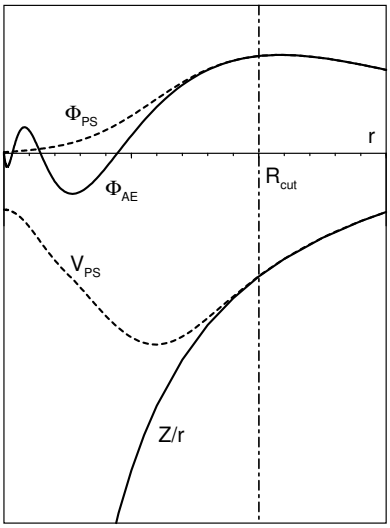

Figure 3. Schematic illustration of an atomic all–electron wave function (solid line) and the corresponding atomic pseudo wave function (dashed line) together with the respective external Coulomb potential and pseudopotential.

removed from the calculation which makes the calculation of energy differences between atomic configurations numerically much more stable.

In principle one might just take the distribution of the core electrons and combine their Hartree potential with the Coulomb potential of the nucleus to an ionic core potential. However, this is not very useful since the valence wave functions still have to maintain their nodal structure in order to be orthogonal to the core states. Much more practical is to replace immediately the ionic core potential by a pseudopotential which will lead to nodeless valence wave functions, as we will show in the following.

3.2 Normconserving Pseudopotentials

Present day pseudopotentials are constructed from ab initio calculations for isolated atoms. Let us assume we have solved the Kohn–Sham equations for a single atom of the chemical species for which we would like to generate a pseudopotential. This can be done easily since due to the spherical symmetry of atoms the wave functions can be written as a product of a radial function and a spherical harmonic. The Schrödinger equation then reduces to one–dimensional differential equations for the radial functions which can be integrated numerically. A typical result for a radial function from such an "all–electron" atom calculation together with the corresponding external Coulomb potential is shown in Figure 3. Our aim is now to replace the effective all–electron potential within a given sphere with radius $R_{\rm cut}$ by a much weaker new potential with a nodeless ground state wave function to the same energy eigenvalue as the original all–electron state which matches exactly the all–electron wave function outside $R_{\rm cut}$ (depicted with dashed lines in Figure 3).

Why should this be possible at all? This can be understood by the following line of arguments. The radial Schrödinger equation for a fixed potential and fixed energy ε (not

necessarily an eigenvalue) to the angular momentum l is a one–dimensional ordinary linear second order differential equation which has two linear independent solutions. However, only one of the two solutions, $\Phi_l(r)$, is regular for $r \to 0$. The logarithmic derivative

$$L_l(\varepsilon) = \left.\frac{\mathrm{d}}{\mathrm{d}r} \ln \Phi_l(r;\varepsilon)\right|_{R_{\mathrm{cut}}} = \frac{\Phi_l'(R_{\mathrm{cut}};\varepsilon)}{\Phi_l(R_{\mathrm{cut}};\varepsilon)} \tag{23}$$

is therefore a well defined function of the energy ε. On the other hand, for a given energy ε and logarithmic derivative L_l at R_{cut} the solution of the radial Schrödinger equation inside and outside the sphere is uniquely defined (save a constant factor). This follows directly from the properties of one–dimensional second order differential equations. However, the solution is only regular for $r \to 0$ if the energy ε and the logarithmic derivative L_l fulfill the relation Eq. (23). From this observation we can conclude that if we modify the potential inside the atomic sphere in such a way that the relation $L_l(\varepsilon)$ is not changed, the wave functions outside the sphere remain unchanged.

For the energy of the eigenstate of our all–electron calculation $\varepsilon_l^{\mathrm{AE}}$ this can be done in the following way: we replace the all–electron wave function Φ_l^{AE} inside the sphere by an arbitrary smooth nodeless function Φ_l^{PS} with the same logarithmic derivative at R_{cut} as the original all–electron function. Since the Φ_l^{PS} is nodeless we can simply invert the radial Schrödinger equation with this new function and with the eigenvalue $\varepsilon_l^{\mathrm{AE}}$ of the all–electron calculation to get the potential that has exactly the required property! In fact, we have a quite large extend of freedom to setup the new pseudo wave function Φ_l^{PS}, and over the last decades many different recipes have been published how it could be done[17–24]. One further important requirement is the so-called normconserving condition. The all–electron and the pseudo wave function inside the atomic sphere must have the same norm to guarantee that both wave functions generate identical electron densities in the outside region. Next to this condition, the additional degrees of freedom in generating a suitable pseudopotential can be employed to make the pseudo wave functions as smooth as possible[25].

Up to now we have reproduced the logarithmic derivative of the effective all–electron potential only for the reference energy $\varepsilon_l^{\mathrm{AE}}$. However, if we change the chemical environment of our atom, the eigenstates will be at a slightly different energy. Therefore, for a pseudopotential to be useful it has to be able to reproduce the logarithmic derivative of the all–electron potential over a whole energy range. The wider this energy range the more “transferable” to other chemical environments is the pseudopotential. As it has been shown, in particular the normconserving condition guarantees such a transferability. Furthermore, the pseudopotential should be as “soft” as possible. By this we mean that the number of plane waves required to expand the pseudo wave functions should be as small as possible. Both properties, transferability and softness, are closely related to the cutoff radius R_{cut} and compete with each other. Low cutoffs give pseudopotentials with a very good transferability. However, increasing R_{cut} makes the pseudopotentials softer. Usually one has to find a compromise between the two requirements. An upper limit for R_{cut} is given by half the distance to the next nearest atom in the configuration for which we want to apply the pseudopotential. If we exceed this value there won’t be any region between the neighboring atoms left where we recover the true all–electron wave functions. Hence, we can not expect anymore to get an accurate description of the chemical bond between the two atoms.

3.3 Fully Nonlocal Pseudopotentials

Since the logarithmic derivative in Eq. (23) depends on the angular momentum l we have to construct a separate pseudopotential $V_l^{\rm PS}(r)$ for each value of l. The full pseudopotential for our atom therefore has to be a nonlocal operator. This is done in the following way:

$$\hat{V}^{\rm PS} = V_{\rm loc}^{\rm PS}(r) + \sum_l V_{{\rm nl},l}^{\rm PS}(r)\,\hat{\rm P}_l \quad , \qquad V_{{\rm nl},l}^{\rm PS}(r) = V_l^{\rm PS}(r) - V_{\rm loc}^{\rm PS}(r) \quad . \tag{24}$$

The pseudopotential $V_l^{\rm PS}(r)$ to one specific angular momentum (usually the highest value of l for which a pseudopotential has been generated) is taken to be the so-called local part of the pseudopotential $V_{\rm loc}^{\rm PS}(r)$. The nonlocal components $V_{{\rm nl},l}^{\rm PS}(r)$ are defined as the differences between the original l–dependent $V_l^{\rm PS}(r)$ and this local part of the pseudopotential. Since all $V_l^{\rm PS}(r)$ are identical outside of $R_{\rm cut}$ the nonlocal components of the pseudopotential are strictly confined within $R_{\rm cut}$. $\hat{\rm P}_l$ is a projection operator which picks out the l–th angular momentum component from the subsequent wave function. By this construction it is guaranteed that when the full pseudopotential operator $\hat{V}^{\rm PS}$ is applied to a general wave function each angular momentum component of the wave function experiences only its corresponding part $V_l^{\rm PS}(r)$ of the potential.

Since the projection operators $\hat{\rm P}_l$ act only on the angular variables of the position vector $\mathbf{r}$ the pseudopotential $\hat{V}^{\rm PS}$ is still a local operator with respect to the radius r. The form (Eq. (24)) is therefore called a semilocal pseudopotential. For numerical efficiency, however, it would be desirable to have the pseudopotential in a fully nonlocal form:

$$\hat{V}^{\rm PS} = V_{\rm loc}^{\rm PS}(r) + \sum_{ij} |\beta_i > B_{ij} < \beta_j| \quad . \tag{25}$$

The $\beta_i(\mathbf{r})$ are suitably chosen projection function which are strictly localized within $R_{\rm cut}$. Kleinman and Bylander[26] have given a prescription how a semilocal potential of the form (Eq. 24)) can be transformed into a fully nonlocal representation. As has been shown by Vanderbilt[27] it is also possible to construct directly from an atomic all–electron calculation a fully nonlocal potential. Basically all present plane–wave–based total energy codes employ pseudopotentials in the form of Eq. (25).

3.4 Vanderbilt Ultrasoft Pseudopotentials

Very difficult to treat within a pseudopotential scheme are all elements with nodeless valence states (in particular those with $2p$ and $3d$ valence electrons). For those elements the pseudo and the all–electron wave functions are almost identical. Since these valence electrons are strongly localized in the ionic core region, many plane waves are required for a good representation of their wave function which often makes calculations for such elements prohibitively expensive.

To circumvent this problem Vanderbilt has introduced a new type of pseudopotentials, the so-called ultrasoft pseudopotentials, in which the normconserving requirement has been relaxed[27,28]. Instead of representing the full valence wave function by plane waves, only a small portion of the wave function is calculated within the Vanderbilt ultrasoft pseudopotential scheme (see dashed line in Figure 4). This allows to reduce substantially the plane wave cutoff energy in the calculations. The price to pay, however, is that the Fourier

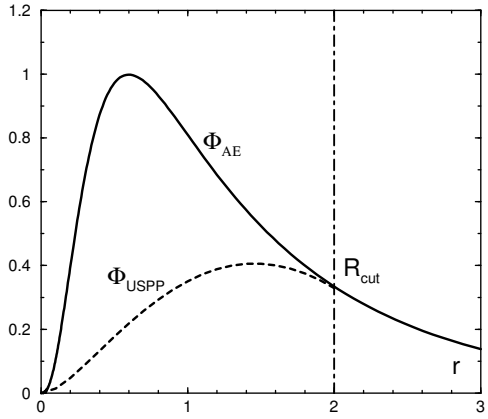

Figure 4. Illustration of a strongly localized valence wave function inside the atomic core region and the modified wave function in the Vanderbilt ultrasoft pseudopotential scheme.

representation of the Kohn–Sham equation becomes more complicated. First, when the electron density is calculated we have to add back the part of the electron distribution which is represented by the difference between the solid and the dashed line in Figure 4 (the so-called augmentation charges). Second, due to the relaxation of the normconserving condition, the Bloch eigenstates $\psi_{\mathbf{k}j}$ will be not orthonormal anymore. An overlap matrix has to be introduced and the eigenvalue problem (Eq. (19)) will transform into a generalized eigenvalue equation. Third, the nonlocal part of the pseudopotential becomes density–dependent. Fourth, due to these modification additional terms in the force calculation have to be evaluated. However, the gain in computational cost by lowering the plane wave cutoff energy outweigh in many cases the additional computational effort which is required by these modifications.

References

1. N.W Ashcroft and N.D. Mermin, *Solid State Physics*, (Saunders College Publishing, Philadelphia, 1976).
2. C. Kittel, *Introduction to Solid State Physics*, (Wiley & Sons, New York, 1976).
3. P.J.H. Denteneer and W. van Haeringen, J. Phys. C: Solid State Phys. **18**, 4127 (1985).
4. W. Pickett, Comput. Phys. Rep. **9**, 115 (1989).
5. M.C. Payne, M.P. Teter, D.C. Allan, T.A. Arias, and J.D. Joannopoulos, Rev. Mod. Phys. **64**, 1045 (1992).
6. D. Marx and J. Hutter, in *Modern Methods and Algorithms of Quantum Chemistry*, ed. J. Grotendorst, (NIC, FZ Jülich, 2000), see `http://www.theochem.rub.de/go/cprev.html`.
7. D.J. Chadi and M.L. Cohen, Phys. Rev. B **8**, 5747 (1973).
8. H.J. Monkhorst and J.D. Pack, Phys. Rev. B **13**, 5188 (1976).
9. J. Moreno and J.M. Soler, Phys. Rev. B **45**, 13891 (1992).
10. C.-L. Fu and K.-M. Ho, Phys. Rev. B **28**, 5480 (1983).

11. M.J. Gillan, J. Phys.: Condens. Matter **1**, 689 (1989).
12. M. Methfessel and A.T. Paxton, Phys. Rev. B **40**, 3616 (1989).
13. P.E. Blöchl, O. Jepsen, and O.K. Andersen, Phys. Rev. B **49**, 16223 (1994).
14. J.C. Phillips and L. Kleinman, Phys. Rev. **116**, 287 (1959).
15. M.L. Cohen and V. Heine, *Solid State Physics, Vol. 24*, (Academic, New York, 1970).
16. W.H. Press, S.A. Teukolsky, W.T. Vetterling, and B.P Flannery, *Numerical Recipes*, (Cambridge University Press, 1992).
17. D.R. Hamann, M. Schlüter, and C. Chiang, Phys. Rev. Lett. **43**, 1494 (1979).
18. G.B. Bachelet, D.R. Hamann, and M. Schlüter, Phys. Rev. B **26**, 4199 (1982).
19. G. Kerker, J. Phys. C **13**, L189 (1980).
20. D. Vanderbilt, Phys. Rev. B **32**, 8412 (1985).
21. N. Troullier and J.L. Martins, Solid State Comm. **74**, 613 (1990).
22. N. Troullier and J.L. Martins, Phys. Rev. B **43**, 1993 (1991).
23. S. Goedecker, M. Teter, and J. Hutter, Phys. Rev. B **54**, 1703 (1996).
24. C. Hartwigsen, S. Goedecker, and J. Hutter, Phys. Rev. B **58**, 3641 (1998).
25. A.M. Rappe, K.M. Rabe, E. Kaxiras, and J.D. Joannopoulos, Phys. Rev. B **41**, 1227 (1990).
26. L. Kleinman and D.M. Bylander, Phys. Rev. Lett. **48**, 1425 (1982).
27. D. Vanderbilt, Phys. Rev. B **41**, 7892 (1990).
28. K. Laasonen, A. Pasquarello, R. Car, C. Lee, and D. Vanderbilt, Phys. Rev. B **47**, 10142 (1993).